Cerebral Cortex Advance Access published November 17, 2008

Cerebral Cortex
doi:10.1093/cercor/bhn205

# Seeing with Profoundly Deactivated Mid-level Visual Areas: Non-hierarchical Functioning in the Human Visual Cortex

Sharon Gilaie-Dotan[1], Anat Perry[2], Yoram Bonneh[1], Rafael Malach[1] and Shlomo Bentin[2,3]

[1]Department of Neurobiology, Weizmann Institute of Science, Rehovot, Israel, [2]Department of Psychology and [3]Center for Neural Computation, Hebrew University of Jerusalem, Jerusalem, Israel

**A fundamental concept in visual processing is that activity in high-order object-category distinctive regions (e.g., lateral occipital complex, fusiform face area, middle temporal+) is dependent on bottom-up flow of activity in earlier retinotopic areas (V2, V3, V4) whose main input originates from primary visual cortex (V1). Thus, activity in down stream areas should reflect lower-level inputs. Here we qualify this notion reporting case LG, a rare case of developmental object agnosia and prosopagnosia. In this person, V1 was robustly activated by visual stimuli, yet intermediate areas (V2–V4) were strongly deactivated. Despite this intermediate deactivation, activity in down stream visual areas remained robust, showing selectivity for houses and places, while selectivity for faces and objects was impaired. The extent of impairment evident in functional magnetic resonance imaging and electroencephalography activations was somewhat larger in the left hemisphere. This pattern of brain activity, coupled with fairly adequate everyday visual performance is compatible with models emphasizing the role of nonlinear local "amplification" of neuronal inputs in eliciting activity in ventral and dorsal visual pathways as well as perceptual experience in the human brain. Thus, while the proper functioning of intermediate areas appears essential for specialization in the cortex, daily visual behavior and reading are maintained even with deactivated intermediate visual areas.**

**Keywords:** cortical selectivity, ERPs, fMRI, prosopagnosia, visual agnosia, visual system

## Introduction

Evidence from anatomical and single unit recording studies in the monkey (Maunsell and Newsome 1987; Felleman and Van Essen 1991; Hubel and Wiesel 1998; Lamme and Roelfsema 2000), as well as more recent human neuroimaging studies (Tootell et al. 1996; Kastner et al. 2001; Lerner et al. 2001; Smith et al 2001; Avidan et al. 2002; see review by Grill-Spector and Malach 2004) suggest a hierarchical flow of information in the visual cortex. Although in a strong form a bottom-up hierarchical model has been challenged (Felleman and Van Essen 1991; Hubel and Wiesel 1998; Schmolesky et al. 1998; Bullier 2001a; Hochstein and Ahissar 2002; Van Essen, 2005), hierarchy is still considered a major anatomical and functional principle in vision. According to this view, a great part of the cortical activity in the visual system flows in a feed-forward manner via parallel pathways in the ventral and dorsal streams (Ungerleider and Mishkin 1982; Van Essen, 2005)—both initiated at V1, and progressing through intermediate regions to more down stream cortical regions. The functional properties of neurons along the visual pathways support such a hierarchical buildup with growing size of receptive fields (e.g., Kastner et al. 2001; Smith et al. 2001), sensitivity that becomes more complex (Hubel and Wiesel 1998; Lerner et al. 2001; Avidan et al. 2002; Grill-Spector and Malach 2004), and increasing response latencies (Schmolesky et al. 1998; Lamme and Roelfsema 2000). At the most complex levels of the unimodal visual system are category-selective areas tuned to global properties of structured object stimuli (lateral occipital complex [LOC], Malach et al. 1995; Grill-Spector and Malach 2004). In addition, some of these areas show selectivity for specific categories (e.g., fusiform face area [FFA] for faces (Kanwisher et al. 1997), and the parahippocampal place area (PPA) or the collateral sulcus (CoS) for places, scenes, and houses (Epstein and Kanwisher 1998; Levy et al. 2001; Hasson et al. 2003; Levy et al. 2004).

Notwithstanding rapid feed-forward bypasses that are exterior to the visual system (from V1 to the pulvinar; Van Essen, 2005; or to prefrontal cortex; Bar 2003, 2006) as well as top-down feedback, the putative hierarchical organization, even in a weak form, suggests that the activity at each cortical stage is driven largely by activity originating from lower levels. Consequently, a disruption in this feed-forward chain of activations should significantly reduce and disrupt the activity downstream.

Indirect support for this hypothesis is provided by rare cases of apperceptive visual agnosia in which object recognition is impaired due to lesions in the lower-level visual cortex (Farah 1990; Cowey 1994; Davidoff and Warrington 1999; Heider 2000). However since most reported cases of acquired visual agnosia are induced by acquired lesions, which are usually diffuse and typically engage more than a single area, their precise neuroanatomical correlates are vague. (Compare with localization of lesions in cases of acquired prosopagnosia; Barton et al. 2002; Bouvier and Engel 2006.) Unfortunately, the few reported cases of developmental object agnosia (case AB; McConachie 1976; De Haan and Campbell 1991), case AL (Joy and Brunsdon 2002), case NM (Duchaine el al. 2003), case TA (Jones and Tranel 2001), as well as the previous report of case LG (Ariel and Sadeh 1996), who is at the focus of the present study, did not include descriptive neuroimaging correlates. To this end, we report here a detailed functional neuroimaging and event-related potentials (ERP) study of LG, a person with developmental (perhaps congenital) rather than acquired object agnosia. These data shed additional light on the possible consequences of disrupting the bottom-up hierarchical flow.

LG demonstrates an extremely rare visual functioning deficiency, which combines severe developmental prosopagnosia with a peculiar form of a more general visual agnosia. Neuroimaging (fnctional magnetic resonance imaging [fMRI]) and electrophysiology studies (pattern-VEP [visual evoked

© The Author 2008. Published by Oxford University Press. All rights reserved.
For permissions, please e-mail: journals.permissions@oxfordjournals.org

potential] and N170) in this person revealed significant visual activation in the striate cortex but with an exceptional functional abnormality that was most prominent in the intermediate levels of the visual processing pathways (from V2 to a region presumed to be V4). The activity in these intermediate areas is profoundly deactivated by any visual stimulus. Interestingly, despite this deactivation, more down stream visual areas remained robustly activated by visual stimulation and partially selective. Specifically, the PPA/CoS and the middle temporal+ (MT+) regions were selectively activated by relevant stimuli. Although the categorical selectivity in ventral-temporal and posterior temporo-lateral visual areas was not entirely normal, the residual higher-order visual activations in the absence of intermediate-levels mediation suggests a highly nonlinear spatio/temporal transfer of information along the cortical hierarchy, in which cortical activity is largely dependent on recurrent "amplification" (Douglas and Martin 2004; Nir et al. 2008a) of cortical activity largely internal to the cortical region (Raichle 2006) rather than being driven by lower-level inputs.

## Methods

### *Magnetic Resonance Imaging*

*fMRI Participants and Setup*

LG and 9 healthy controls (mean age 31.33 ± 2.57, 4 women) participated in the fMRI experiments. All the controls had normal or corrected-to-normal vision. Written informed consent to participate in the experiments has been obtained from all the fMRI participants according to the Tel-Aviv Sourasky Medical Center "Helsinki" committee that approved the experimental protocol. Participants were scanned in a 1.5 T Signa Horizon LX 8.25 GE scanner (GE Healthcare, Piscataway, NJ).

Blood oxygenation level–dependent (BOLD) contrast was obtained with gradient-echo echo-planar imaging (EPI) sequence with time repetition = 3000 ms, time echo = 55 ms, flip angle = 90°, field of view 24 × 24 $cm^2$, matrix size 80 × 80. The scanned volume for the controls contained 17 nearly axial slices covering their entire visual cortex (see Hasson et al. 2003, for more details), and 24–25 nearly axial slices for LG in order to cover his entire cortex (via a standard head coil). Slice thickness was 4 mm with 1 mm gap with an in-plane resolution of 3 × 3 $mm^2$.

*fMRI Experiments*

The fMRI experiments are described below, and further details can be found elsewhere (Levy et al. 2001; Lerner et al. 2002; Hasson et al. 2003; Avidan et al. 2005).

*Retinotopic mapping.* As described earlier (Levy et al. 2001, 2004) the representations of the vertical and horizontal visual field meridians were mapped to delineate borders of retinotopic areas (Sereno et al. 1995; DeYoe et al. 1996; Engel et al. 1997). This mapping was based on 1 scan per participant for the control participants and 2 scans for LG. The experiment was block-designed and included 4 stimulus-location conditions (up, down, left, and right), each condition repeated four times. Blocks lasted 18 s and were interleaved with 6-s blank periods. The stimuli were triangular wedges at the upper or lower vertical meridians or at the left or right horizontal meridians. Each block consisted of wedges oriented to only one direction that appeared consecutively, for 250 ms each. Subjects were instructed to fixate a small central cross throughout the experiment. The wedges consisted of colored copies of objects superimposed on colored textures and subtended a visual angle of 9.5° from the fixation cross to the periphery (following the direction of the wedge), and their width reached a maximal visual angle of 8° at the most peripheral point.

*Category-selectivity mapping.* This category-localizer experiment (described in Hasson et al. 2003 as the "Face, Building, and Object Localizer experiment") was aimed at delineating category-selective regions in high-order visual cortex. It was run once on each control participant and twice on LG. This block-designed experiment included 4 stimulus conditions (faces, houses, objects, and patterns), each condition repeated seven times in pseudorandom order. Blocks lasted 9 s and were interleaved with 6-s fixation periods. The entire experiment lasted a total of 450 s. Block consisted of nine images of the same category, each displayed for 800 ms followed by a 200-ms blank screen. All stimuli were line drawings subtending a visual angle of 12° × 12°. The task was a 1-back same or different repetition detection task without overt responses (in order to eliminate head movements). One or two consecutive repetitions of the same image occurred in each block. LG was instructed to press a button following each stimulus in the 1-back task in order to verify his ability to detect the stimuli in the scanner.

LG was also scanned in two additional category-localizer experiments. One was identical in design and format to the line-drawing version but using grayscale photographs instead of the line drawings. The other category-selectivity localizer experiment presented category-related video clips in a block-designed manner. In this experiment, each block lasted 15 s during which a clip was presented continuously. Based on their content, the clips formed four conditions: close-ups of people in various situations ("faces"), navigation of the camera through open fields ("navigation"), navigation through city buildings ("buildings"), and objects from different categories (tools, musical instruments, furniture, kitchenware, etc..; "objects"). Each condition was repeated 8 times with different clips at each repetition. The entire experiment lasted 12 min. Blocks were separated by a 6-s gray blank screen. The clips subtended a visual angle of $21°_{width} \times 17.3°_{height}$. LG was instructed to watch the movie-clips passively (for additional details see Avidan et al. 2005).

*Motion-selectivity mapping.* This experiment (as described earlier in Hasson et al. 2003) was aimed at delineating motion-sensitive regions in the visual cortex (e.g., MT+). The experiment included 2 conditions ("static" and "motion") which were repeated 8 times each, in a block-designed fashion. Blocks lasted 18 s each, and were interleaved with 6-s fixation periods. The stimuli consisted of low contrast rings (6% contrast for all participants, 2 cycles/degree and a duty cycle = 0.2) surrounding the fixation point and forming a maximal visual angle of 16° x 16°. In the motion condition the rings appeared as expanding or contracting (for 2 s in each direction of motion), while in the static condition rings were displayed for 3 s each in a consecutive manner (hence not causing motion perception). Subjects were instructed to maintain fixation throughout the experiment). The experiment lasted 420 s.

*Completion experiment.* The completion experiment was block-designed and included 3 conditions: "whole" (stimuli were presented in full view), "grid" (grid of green vertical stripes was superimposed on the image hiding parts of it, see details below) and "scrambled" (the horizontal order of the visible parts of the images (behind the grids) was re-shuffled; see example of stimuli in Fig. 1*C*). Each condition was repeated in seven blocks in a pseudorandom order. A block lasted 9 s, and consisted of 18 different images of a basic level category of animals, (e.g., "dog," "cat," "giraffe") each image displayed for 500 ms. The blocks were separated by 6 s during which a blank screen was presented. The stimuli were line drawings subtending a visual angle of $14°_{width} \times 12°_{height}$ (see examples of the stimuli in Fig. 1*C*). The grid consisted of green vertical stripes (each stripe 1.2 × 12°, duty cycle = 0.5), with the borders smoothed. Participants were instructed to silently name the images at the basic category level and guess the name if the image was not recognizable (see Lerner et al. 2001 for more details). Stimulus recognition was tested outside the magnet in a similar experimental design using the same stimuli as those used during the scan. Control participants were tested about 4 weeks after the fMRI scan (to avoid priming), while LG was tested immediately after the scan.

During this stimulus recognition test outside the scanner, the instructions were to name out loud the animal images as specifically

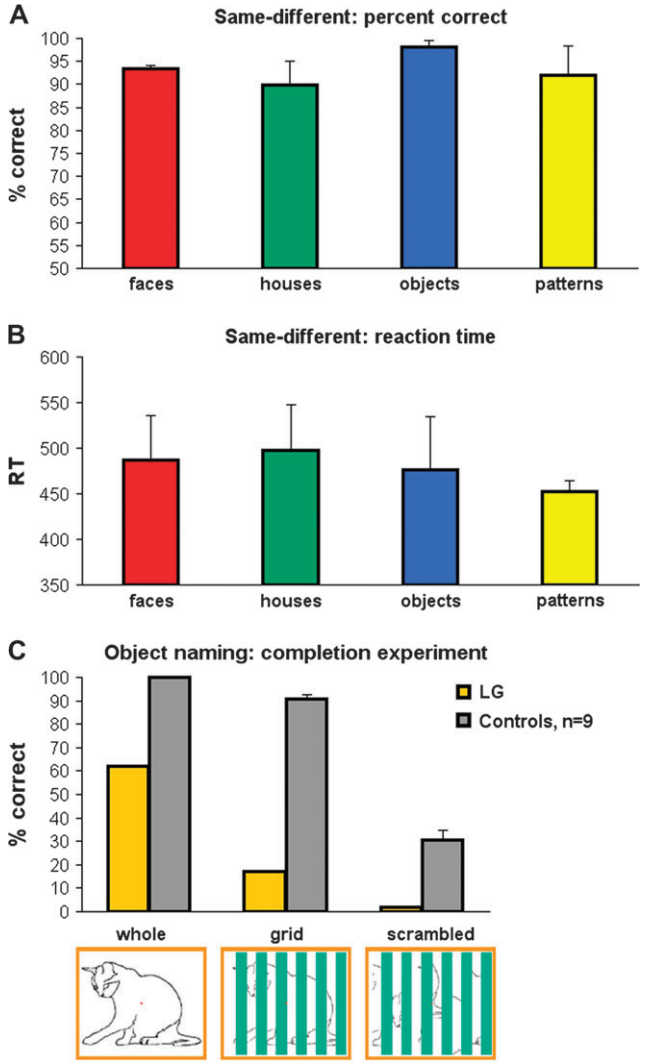


**Figure 1.** fMRI-related behavior in LG. (*A*, *B*) LG's average performance in the scanner in a 1-back same-different comparison task from the 3 category-selectivity scans (2 scans with line-drawing stimuli, 1 scan with grayscale pictures stimuli, see Methods for more details). Responses were collected via a response box. (*A*) percent correct, (*B*) reaction time. (*C*) LG's object naming performance (in percent correct, compared to 9 healthy controls) as measured immediately after the scan outside the scanner. The stimuli consisted of the stimuli from the completion experiment (Lerner et al. 2001), see Methods and Results for more details). Yellow bars indicate LG's performance, gray bars, controls. An illustration of the stimuli of the different conditions is given below the bars. Note that LG performed well above chance in the comparison task (*A*, *B*), while his performance was significantly impaired in the naming task (*C*). In the completion experiment (*C*), even though LG's performance was already below controls in the whole condition (controls: 100 ± 0%, LG: 62%), his performance dramatically dropped when parts of the image were occluded by bars (grid: controls: 90.8 ± 1.2%, LG: 17%; scrambeled: controls: 30.7 ± 12%, LG: 2%).

as possible. Performance was measured as the percentage of correct naming either at the basic (e.g., "monkey") or at subordinate levels (e.g., "gorilla", "chimp"). The order of stimuli was the same as that in the fMRI scan. For the controls, each stimulus was presented for 500 ms, followed by a 1500-ms blank during which the overt naming of the image has been recorded. For LG each stimulus was presented for 500 ms, but followed by a 3000-ms blank screen to allow more time for recognition and naming.

### *fMRI Data Preprocessing and Analysis*

fMRI data were analyzed with the *BrainVoyager* software package (R. Goebel, Brain Innovation, Maastricht, The Netherlands) and additional in-house software. The first two or three images of each functional scan were discarded. The functional images were superimposed on 2D anatomic images and incorporated into the 3D data sets (see structural MRI below) through trilinear interpolation. The complete data set was transformed into Talairach space (Talairach and Tournoux 1988). Preprocessing of functional scans included 3D motion correction, slice scan time correction, linear trend removal and filtering out of low frequencies up to 10 cycles per experiment.

A general linear model (Friston et al. 1995) was fit separately to the time course of each individual voxel in each experiment according to the experimental protocol. The model coefficients for each voxel were determined so that the error term between the model's prediction and the measured voxel time course is minimized (Least Squares method). The analysis was performed independently for each individual voxel. A *t* test between coefficients of different conditions was applied to determine a voxel's activation pattern. The voxel's *P* value was determined as the *P* corresponding to the resulting *t* value of the *t*-test. Visually activated voxels (in all the category-selectivity experiments and in the completion experiment) were determined by contrasting for every voxel the coefficients of all the experimental conditions against fixation baseline and taking into account the voxel's error term; motion-selective voxels were determined by contrasting the motion coefficient against the static coefficient. In order to contrast faces versus buildings and common objects the coefficient of the face predictor was compared to the average of the building and common object predictors (for further details see Hasson et al. 2003; Avidan et al. 2005).

Regions of interest (ROIs) were determined for each subject separately based on a minimum cluster size of 6 functional voxels. The V1 ROI comprised the visually activated regions within V1 retinotopic boundaries. For LG the V1 ROI was determined in the same way as for the control participants since the V1–V2 retinotopic boundary was evident from the retinotopic mapping experiment (see Supplementary Material for more details). The V1 activation thresholds for controls were set at $P < 0.05$ while for LG at $P < 0.001$. ROIs of intermediate retinotopic regions were determined for control participants as the activated regions within V2–V3 retinotopic boundaries. For LG, the retinotopic boundaries beyond the V1–V2 boundary were not detectable from the retinotopic mapping experiments; therefore, the ROIs of intermediate regions were defined as the negative patches corresponding anatomically to the controls' intermediate retinotopic ROIs. The Lateral Occipital (LO) ROIs (from which the time courses displayed in Figs 4 and 5*B* were sampled) were defined for controls as well as for LG as a visually activated patch in the lateral occipital aspect of the cortex, which corresponded anatomically to the LOC location (Malach et al. 1995; Grill-Spector and Malach 2004). The MT+ ROI was determined as the motion-selective region (motion > static) in the middle temporal cortex, located ventrolaterally, just posterior to the meeting point of the inferior temporal sulcus and the lateral occipital sulcus in the vicinity of the middle occipital gyrus/sulcus.

*fMRI time-course analysis.* This analysis was based on sampling from ROIs that were determined for each subject separately. We sampled the time courses of activation during the category-selectivity experiment separately in V1, the intermediate regions and LO, and then computed the percent signal change in each area compared to the blank period preceding it. Repetitions of each condition were then averaged for each time point along the block. Right and left hemisphere ROI time courses were combined by a weighted average only when no significant differences were found between them. Finally, for each ROI (V1, intermediate and LO) and for each condition the time course functions were averaged across the control participants (Fig. 4, left column). For LG the analysis was similar to that of the controls and was based on the 3 scans of the category-selectivity experiment (twice with the line-drawing version—like controls, and once with gray-scale images). For each of LG's ROIs (V1, intermediate, and LO) the time course in Figure 4 (middle and right columns) is the average across the 3 runs. As with the controls, the left and right hemisphere ROIs in LG were averaged only if no significant difference between them was found; otherwise they are presented separately. LG's time courses from the category-related movie-clip experiment, completion experiment (Fig. 5*A*,*B*) and

the motion-selectivity mapping experiment (Fig. 8) were calculated in the same manner as described above; the percent signal change was computed relative to the blank period preceding it.

*Structural MRI*

A whole-brain spoiled gradient (SPGR) sequence was acquired for each participant including LG (field of view 240 × 240 $mm^2$, matrix size 256 × 256, slice thickness 1.2 mm, 124 axial slices) to allow accurate cortical segmentation, reconstruction, and volume-based statistical analysis. In addition, high-resolution (1.1 × 1.1 $mm^2$) $T_1$-weighted anatomic images of the same orientation and thickness as the EPI slices were also acquired to facilitate the incorporation of the functional data into the 3D Talairach space (Talairach and Tournoux 1988).

The cortical surface was reconstructed from the 3D SPGR scan. The procedure included segmentation of the white matter using a grow-region function, the smooth covering of a sphere around the segmented region, and the expansion of the reconstructed white matter into the gray matter. The surface of each hemisphere was then unfolded, cut along the calcarine sulcus and additional predefined anatomical landmarks on the medial side, and flattened.

### *Electrophysiology*

*Pattern-VEP*

The stimuli and experimental procedures in the VEP study were identical to those used by Di Russo et al. (2002), who verified their intracranial sources. The stimuli consisted of circular checkerboards sinusoidally modulated in black and white, and were presented binocularly one at a time in randomized sequences separately to each of the 4 quadrants of visual fields at a rate varying between 250 and 550 ms. Stimulus positions were centered along an arc that was equidistant (4°) from a central fixation point and located at polar angles of 25° above and 45° below the horizontal meridian. Each stimulus had a diameter of 2° of visual angle and a spatial frequency modulation of 4 cycles/degree. These stimuli were flashed for 50 ms duration against a gray background (20 cd/$m^2$) that was isoluminant with the mean luminance of the checkerboard pattern, which itself was modulated at a contrast of 80%. In order to maintain fixation, all participants were instructed to focus on a small fixation point and press a button each time its luminance changed.

Whereas each of 6 control participants was tested once, LG was tested twice in sessions separated by three weeks. The VEP elicited in each of these sessions were very similar and therefore averaged for further analysis.

*N170*

The stimuli of the N170 experiment were based on photographs of different faces, different (analog) watches and different flowers, all stimuli equated for luminance and RMS contrast. Seen from a distance of approximately 60 cm they occupied 9.5° × 13° of the visual field (10 cm × 14 cm), and were presented at fixation. The stimuli were presented one at a time in random order for 700 ms with ISIs varying between 500 and 1250 ms. Participants were instructed to press a button each time a flower appeared.

*Electroencephalography Data Analysis*

The electroencephalography (EEG) analog signals were recorded continuously by 64 Ag–AgCl (128 in the VEP experiment) pin-type active electrodes mounted on an elastic cap (Electrocap International, Eaton, Ohio) according to the extended 10–20 system, and from two additional electrodes placed at the right and left mastoids, all reference-free. Eye movements, and blinks, were monitored using bipolar horizontal and vertical EOG derivations via two pairs of electrodes, one pair attached to the external canthi, and the other to the infraorbital and supraorbital regions of the right eye. Both EEG and Electrooculogram (EOG) were sampled at 1000 Hz using a Biosemi Active II digital 24-bits amplification system (Amsterdam, The Netherlands) with an active input range of −262 mV to +262 mV per bit without any filter at input. The digitized EEG was saved and processed off-line. Raw data was 1.0 Hz high-pass filtered (24 dB) and re-referenced to the tip of the nose. Artifact free data was then segmented into epochs ranging from −250 ms before to 800 ms after stimulus onset for all conditions, and the segments were averaged separately for each condition. For each subject, the peak amplitude of the N170 was determined as the most negative peak between 150 and 200 ms.

## Results

### *Case Description*

LG is a 21 years old male (he was 19 years old at the time of testing) who was first diagnosed with object recognition problems in early childhood (Ariel and Sadeh 1996). He does not suffer from any neurological disease. No discernible structural cortical abnormality was detected in the examination of LG's structural high-resolution brain images by an expert neuroradiologist who was blind to LG's condition (see Methods for details). We examined his visual and perceptual abilities in an extensive series of normative as well as specially designed tests. Here we present a synopsis of the major findings.

### *Low-Level Vision*

Although objective clinical ophthalmologic examination did not indicate abnormal visual acuity (no refractive errors or optical correction were found necessary or effective), his visual acuity measured in a standard optometric ETDRS chart from 3 m was low, 0.5–0.6 LogMAR in both eyes. In addition we found that a significant part of the acuity deficit was due to crowding (~0.3 log units, which is larger than normal as measured with crowded and uncrowded displays of tumbling E patterns (Bonneh et al. 2004). A conspicuous difficulty with dot grouping suggested problems of visual integration that were further investigated. Two tests suggested abnormal early integration mechanisms. In a contour-in-noise card test (Kovacs et al. 1999), his performance was at the level of 5–6 year olds (threshold spacing ratio of ~1); in a lateral masking experiment (Polat and Sagi 1993) he showed no collinear facilitation, which also indicates impairment in local integration mechanisms. In contrast, he performed normally on the standard stereo-vision test (Randot, Stereo Optical Co., Inc). His color vision was perfect when tested with Ishihara plates for color blindness, albeit his response to each plate was slower than usual, probably reflecting his impaired identification of the number shapes. His contrast sensitivity function as tested by VSG Version 4.02 (Cambridge Research Systems, Ltd., 1995) was normal for his age, and when measured with full-field sinusoidal gratings in a temporal two-alternative forced choice procedure was in the normal range below 9 cycles/degree, but lower than normal for 9 and 18 cycles/degree. Additional insights about his visual performance are displayed in Figure 1*A,B*.

### *High-Level Vision and Object Recognition*

LG's high-level vision is peculiar with islands of normal or close to normal performance in some tests but extremely deficient performance in others. He functions as a completely independent adult (works, knows his way around indoors and outdoors), his reading ability is seemingly normal (but see below), and he finished high school successfully. Informally, the way he describes his problems is that "*looking at objects further than about 4 m, I can see the parts but I cannot see them integrated as coherent objects, which I could recognize; however, closer objects I can identify if they are not obstructed; sometimes I can see coherent integrated objects without being able to figure out what these objects are.*"

Indeed, the characteristics of his problems, even at a short viewing distance, are evident, for example, when comparing his performance on the Boston Naming Test, which was within normal range (45 correctly labeled objects out of 54, with all failures explained by cultural factors) and his very weak performance in the Hooper Visual Organization Test (12.5 points out of 30, a score categorized as "very high probability of impairment"). Similarly, his performance with the minimal feature match (Birmingham Object Recognition Battery [BORB-7; Riddoch and Humphreys 1993]) was errorless while his ability to disentangle superimposed line drawings (Birmingham Object Recognition Battery [BORB-6; Riddoch and Humphreys 1993]) was deficient. He performed better with simple geometrical shapes and had a conspicuous difficulty with letters and more complex line drawings. This difficulty was reflected both by errors (e.g., 11 errors out of 36 superimposed triples of letters [108 letters altogether]) and particularly by extremely long RTs—even for the correctly identified trials. The ratio between the RTs of overlapping stimuli compared with RTs of isolated stimuli was three times the ratio of the normal mean. Finally, being presented with Kanizsa figures he easily identified all patterns except a Star of David, which he only recognized after tracing the pattern with his finger. Additional completion deficiencies are evident in object naming results presented in Figure 1*C*.

### *Reading Performance*

LG is a passionate reader both in English and Hebrew, albeit he keeps the text at a distance of about 15–20 cm from his eyes. Formally tested he was able to identify letters, words, and text even if slightly masked, but he was unable to identify individual words under heavy pattern masking, although the same words have been accurately identified by 10 normal viewers.

### *Face Processing*

LG's face processing is extremely impaired. In the Benton Facial Recognition Test (Benton et al. 1983), he was able to match only 33 out of the 54 faces, a score that places him in the severely impaired group. In the Warrington's Face/Word Recognition Test (Warrington 1984) he correctly selected 47 words out of the 50 trials whereas only 37/50 faces. This discrepancy between words and faces, places him in the lowest 5 percentiles of the normal distribution. In the Cambridge Face Memory Test (Duchaine and Nakayama 2006) he was correct in only 34 out of 75 trials, which is 6 points less than the average norm of individuals with congenital prosopagnosia and significantly below the normal mean performance (58/75). When tested with specially designed tests of face identification, he was able to identify only 5 out of 53 famous faces (compared with an average of 40/53 in an age-matched control group of Israelis). Dramatically he was unable to identify his parents, his sister, or himself, in photographs in which the hairline has been eliminated. In contrast, he was better at identifying famous buildings (11/17), even some that he previously knew only from pictures such as the Golden Gate Bridge or the Statue of Liberty. Similarly, he was fairly accurate at identifying pictures of familiar places in his neighborhood and town (18/25).

Interestingly, in contrast to other developmental prosopagnosics (Behrmann et al. 2005; Bentin et al. 2007) LG's performance in a test of local and global processing using hierarchical letters (Navon 1977) showed the normal pattern. RTs were within normal range using both English and Hebrew letters, showing considerable global interference in the local task and much attenuated local interference in the global task.

### *Handedness and School History*

We assessed LG's handedness with the Edinburgh Handedness Inventory (Oldfield 1971). LG was found strictly right-handed (9 activities were indicated as executed by right hand, while 1 activity was not answered (Broom [upper hand]) due to a probable lack of experience with this activity.

LG finished high school with above-average grades, and he successfully passed all the Israeli matriculation examinations and has an Israeli matriculation certificate which is the key to higher education in Israel.

### *Imaging and Electrophysiology Experiments*

We examined the functional organization of LG's visual cortex in light of existing knowledge using fMRI retinotopic mapping (Tootell et al. 1996; Halgren et al. 1999; Grill-Spector and Malach 2004), motion-selectivity mapping (Tootell et al. 1996; Huk et al. 2002; Hasson et al. 2003), and category-selectivity mapping (Kanwisher et al. 1997; Epstein and Kanwisher 1998; Halgren et al. 1999; Levy et al. 2001; Hasson et al. 2003). An additional visual experiment was run on LG (the "completion experiment"; Lerner et al. 2001). In addition to fMRI we examined the temporal aspects of his visual activations by recording checkerboard VEP (Di Russo et al. 2002) and selectivity for faces recording the N170 ERP component (Bentin et al. 1996, 1999, 2007). In addition, we directly compared LG's cortical activation with healthy controls (9 for fMRI, 6 for VEP, and 24 for N170).

### *fMRI-Related Behavioral Performance*

LG's behavioral performance in the magnet for the 1-back same-different comparison task are displayed in Figure 1*A* and *B*. As can be seen, despite his visual agnosia, his performance was well above chance (more than 90% correct for all conditions), and his reaction times in this task were around 450–500 ms on the average. In contrast to the one-back comparison task, his animal recognition ability in the completion experiment was remarkably low even for images presented in the unobstructed view condition (Figure 1*C*). Although the performance of the control participants was measured about a month after the scan (in order to avoid priming) and they had only 1500 ms to respond to each image, their naming accuracy was significantly higher than LG's naming performance, who was tested immediately after scanning and was given twice as much time to respond. In particular, the only picture that he identified in the scrambled condition was based on local cues (the spines of the "porcupine"). Interestingly, LG mentioned that he might have performed better if he had more time for the task.

### *Visual Cortex Activations and Deactivations*

LG's V1 visual activation patterns, as revealed by fMRI in the category-localizer experiment, showed a robust activation level, not different in amplitude from that typically found in normal individuals (Fig. 2; see further details below). (For further details about LG's V1 definition, and additional retinotopic delineations and eccentricity mappings in LG see Supplementary Material.) In contrast, a striking *deactivation*

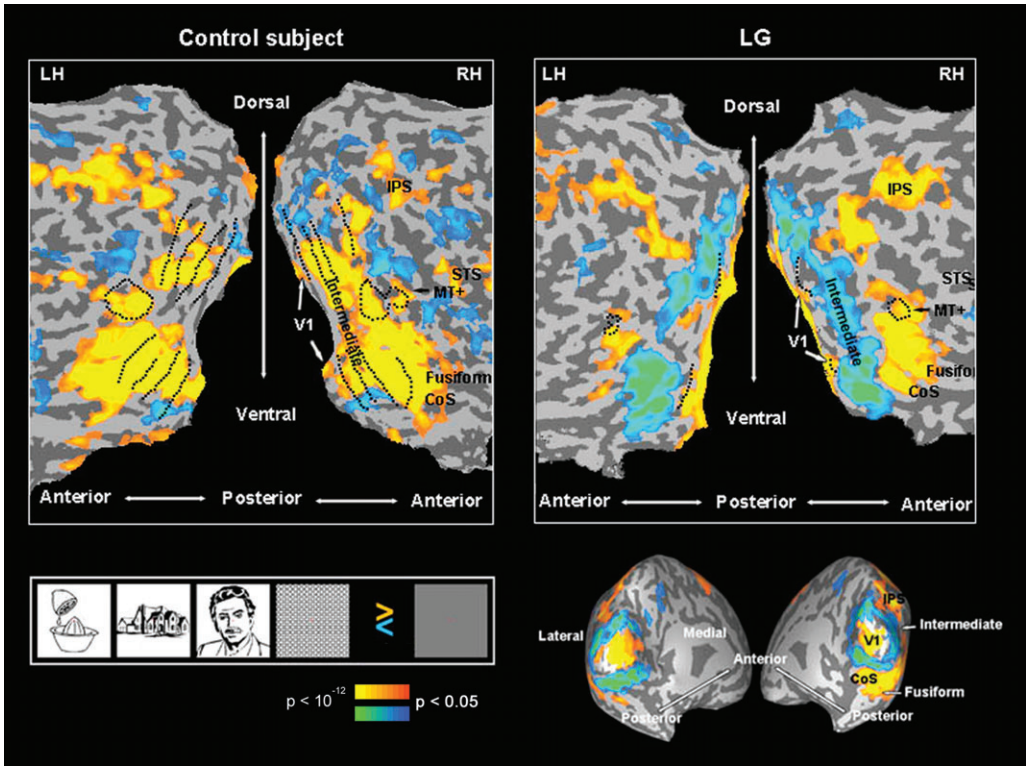


**Figure 2.** Visual activation: LG versus control. Left: typical control subject; right: LG, flattened and inflated cortical sheet. Yellow to orange represent visually activated voxels compared to fixation baseline, blue to turquoise represent visually deactivated voxels compared to fixation baseline. V1, primary visual area; CoS, colateral sulcus; IPS, intraparietal sulcus; STS, superior temporal sulcus; MT+, middle temporal motion-sensitive region. RH, right hemisphere; LH, left hemisphere. Black dotted lines represent retinotopic borders and MT+ border (defined in separate experiments for each subject).

was found at intermediate retinotopic areas, anatomically corresponding to V2, V3 and perhaps even to V4. While, as expected, the intermediate retinotopic areas were activated in controls significantly above baseline by all types of visual stimuli ($P < 0.005$, random effect [RE], $n = 9$), the ventral and dorsal aspects of LG's intermediate retinotopic regions were significantly deactivated by all types of visual input ($P < 10^{-5}$, peak voxel with $P < 10^{-37}$). Furthermore, despite the strong deactivation in V2–V3/VP, the activity of MT+, ventral-temporal regions, and dorsal intraparietal sulci (IPS)–related regions in response to all visual stimuli showed a robust activation which was significantly above baseline ($P < 10^{-5}$, peak voxel with $P < 10^{-37}$) similar in magnitude to that observed in the control participants ($P < 0.01$, RE, $n = 9$). The ventral-temporal regions that were activated in LG correspond anatomically to the LOC (Malach et al. 1995; Grill-Spector and Malach 2004), perhaps also including V4. The individual activation maps (of the controls and LG) are displayed in Supplementary Figures 1 (flattened maps) and 2 (a nonflattened anatomical view). Next, we examined the significance of difference between the above pattern of effects in LG and controls and their reproducibility across experiments, tasks and block cycles. (A full cycle in a block design experiment includes the period of the "ON" stimulus and the "OFF" stimulus period following it.) Reproducibility across different block cycles addressed the possibility that the difference between LG and controls was only a reflection of delayed hemodynamic response in the intermediate regions [especially, when the "on" and "off" portions of the block cycle are very similar, e.g., 9 s "on," 6 s "off"].). These analyses were run separately for the right and left hemisphere, which also enabled assessment of possible hemispheric differences.

The *anatomical expanse of activated V1 cortex* in LG (over the 3 localizer runs) was within the range of the control group (left hemisphere: LG: 1052 ± 826 mm$^3$ [SD]; control group: 1044 ± 345 mm$^3$ [SD]; right hemisphere: LG: 930 ± 490 mm$^3$ [SD] vs. 1049 ± 636 mm$^3$ [SD] for the control group) and there were no interhemispheric differences ($P = 0.256$, paired one-tailed *t*-test for activated voxels of $P < 0.05$; $P > 0.35$ for activated voxels of $P < 0.001$). Supplementary Figures 1 and 2 present the expanse of activated visual cortex in each of the control subjects and reveal the inter-subject variability with respect to the activation patterns in the vicinity of the occipital pole (Stensaas et al. 1974; Andrews et al. 1997; Dougherty et al. 2003; Adams et al. 2007; Amunts et al. 2007). The *average V1 time courses* across control participants is represented in Figure 4 in the top-left panel. The average time courses of LG's V1 (averaged across 3 experimental runs and corresponding to the activation maps of Fig. 2 and Fig. 3*A*,*B*), are displayed in Figure 4 (left V1: top middle panel, right V1: top right panel; see Methods for more details). Using these time courses we further examined the *activation amplitude in LG's V1* as compared to control participants (for each of the experimental conditions separately). The activation amplitude in LG's V1, did not deviate significantly from control in the left hemisphere (LG's amplitude distance from control's mean amplitude given in SD was: faces: –0.02 SD, houses: 1.54 SD, objects: 1.05 SD, patterns: 0.95 SD). However, LG's V1 activation amplitude in

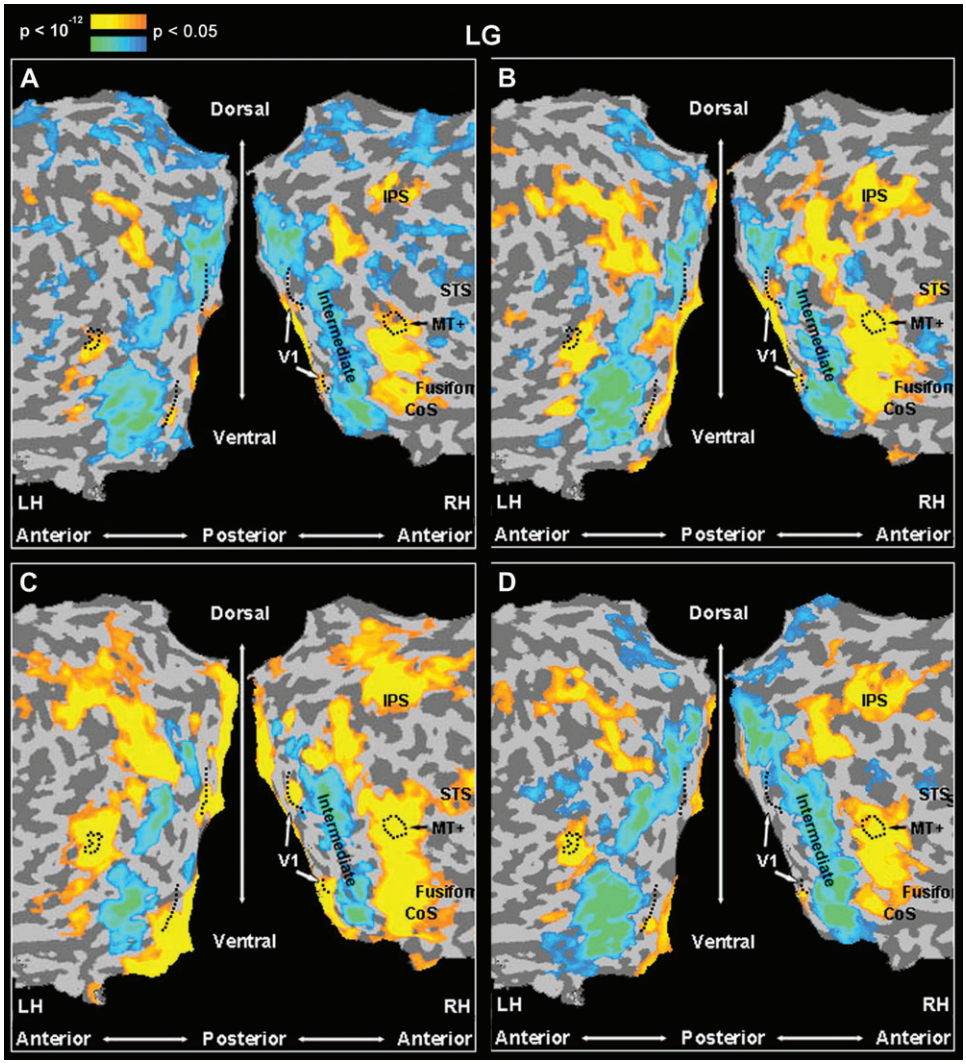


**Figure 3.** Reproducibility of the visual response patterns of activations and deactivations in LG. Same presentation format, anatomical landmarks and statistical significance as in Figure 2, LG, flattened cortical representation. (*A*) LG's visual activation map in a different run of the same experimental protocol as in Figure 2. (*B*) A different run of the same experiment as in Figure 2, with gray-scale images as stimuli. (*C*) LG's visual activation map (fourth run) to an experimental protocol (Avidan et al. 2005) similar to that presented in Figure 2, viewing colored video clips of different categories. (*D*) LG's visual activation map in the completion experiment (Lerner et al. 2001). Note that the activation – deactivation pattern in LG's visual system is replicated in different scans with various experimental stimuli (line drawings, *A*, *D*; gray-scale pictures, *B*; and movie-clips, *C*), different task demands (panels *A* and *B*: same-different 1-back comparison, panel *C*: free viewing, panel *D*: silently naming the image without overt speech), and different block durations (panels *A*, *B*, and *D*: 9-s blocks with fixation periods of 6 s, panel *C*: 15-s blocks with fixation periods of 6 s).

the right hemisphere was higher than in the left and actually higher than in the control group (1.45 SD, 2.25 SD, 4.36 SD, 1.62 SD higher than the control's mean for, faces, houses, objects, and patterns, respectively). This effect is clearly observed through the time course displayed in Figure 4 (upper row). As can be seen there, LG's right V1 was activated to a higher extent than the left in all conditions. A two-way ANOVA of the amplitude with hemisphere (left, right) and condition (objects, faces, houses, patterns) as independent factors showed in LG a significant main effect of hemisphere ($F_{1,16}$ = 7.07, $P$ < 0.02), no effect for condition ($F_{3,16}$ = 2.52, $P$ = 0.095), and no interaction ($F_{3,16}$ < 1.0, $P$ > 0.99). When examining more subtle differences between LG and controls along the time course of each experimental condition, LG's activation in the left hemisphere did not deviated more than 2SD from the control mean except for the 12-s time point after stimulus onset for the objects and houses conditions only. In the right hemisphere the time course of LG's activation for objects and houses deviated from controls (objects between 6 and 12 s and for houses between 9 and 12 s after stimulus onset). To summarize, LG's V1 activation showed activation amplitude and anatomical extent that was within the normal range in the left hemisphere, and was even higher than normal in the right hemisphere. As to stimulus selective responses, they appeared mostly normal with the exception of object and house responses at specific time points. However, it should be emphasized that these measures were not exhaustive and clear abnormalities may have still existed in LG's V1 functional profile.

In order to determine the reliability of the deactivation effects in LG's intermediate cortex, we examined how consistent this pattern was across the various experiments (Fig. 3). Each panel in Figure 3 represents a map of the activation and deactivation patterns of LG's visual cortex in a different visual experiment, contrasting all visual blocks with

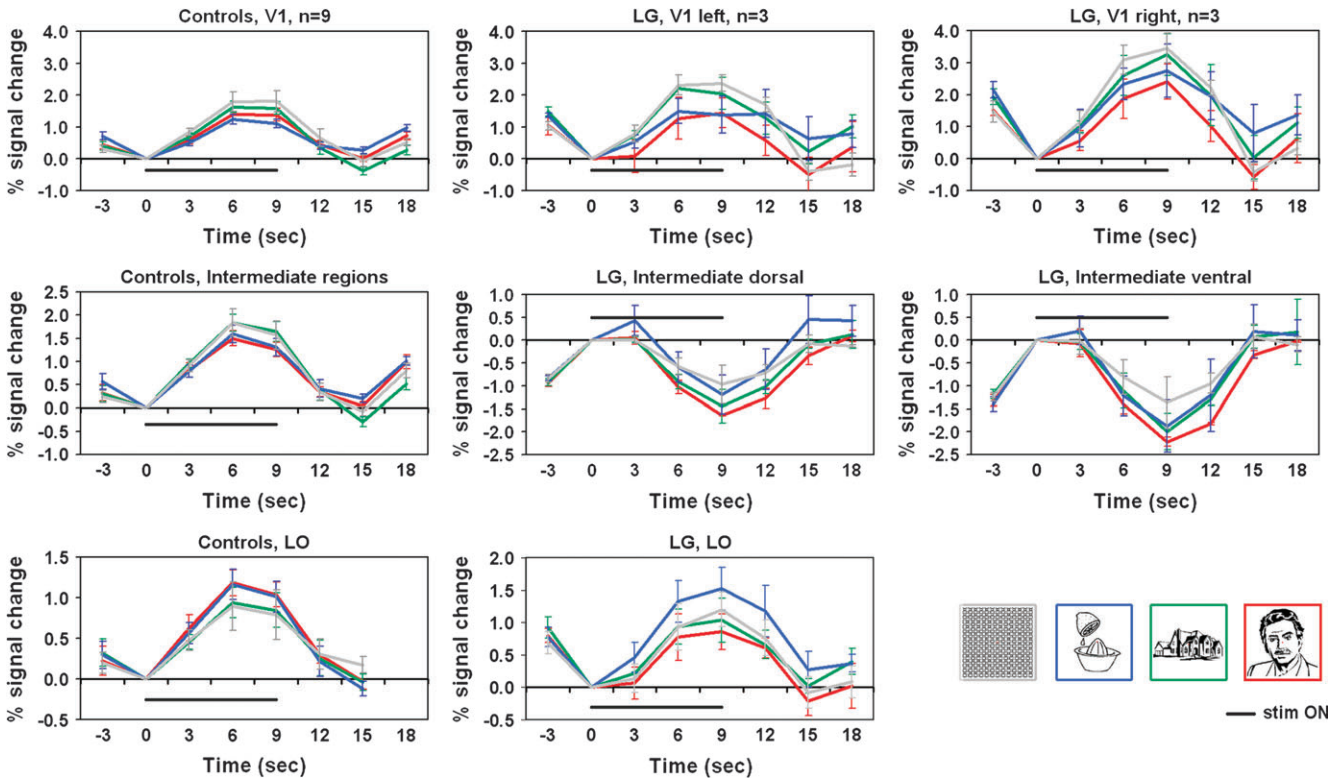


**Figure 4.** Regional time courses: LG versus controls. Average time courses of the controls ($n = 9$) are presented in the left most column; LG's average time courses (sampled from the 3 category-localizer runs he underwent) are presented in the middlle and right columns. The V1 average time courses are displayed in the top row (LG's right and left hemispheres are presented seperately since the right hemisphere was significantly different from both the left hemisphere and from the controls (see Results for details). V1 sampled regions were determined for LG as well as for controls according to activated patches within V1 retinotopic boundaries. Time courses sampled from intermediate-level regions are displayed in the middle row (LG's ventral and dorsal aspects are presented seperately since a significant difference was found between them; no inter-hemisphereic difference was found). Intermediate level regions were determined for controls based on retinotpic borders, so that the sampling was based on activated patches within V2–V3 regions. For LG, intermediate regions were sampled from the deactivated patches in the corresponding anatomical location of V2–V3 in controls. LO related time courses (sampled from the visually activated regions in the anatomical location of LO for both LG and controls) are displayed in the bottom row. The average response to the faces condition is indicated by the red curve, to houses in green, to objects in blue, and to the patterns condition in gray. Stimulus "ON" is indicated by a black line. Error bars denote SEM. Note the prominent deactivation to each of the categories in LG's intermediate areas (middle row). For more details see Methods and Results.

the baseline condition (blank screen). These experiments included different stimuli types, different tasks, and different block cycles. Despite these differences, across all conditions we found a clear and anatomically consistent deactivation throughout LG's intermediate cortex. In contrast, V1, on the one hand, and MT+ as well as down stream areas in the ventral and dorsal pathways of the visual cortex, on the other hand showed a robust activation level significantly above baseline. This deactivation effect of intermediate cortex can also be seen through the average time courses of those regions in the various experiments (see Fig. 4, LG intermediate dorsal and ventral panels; Fig. 5*A*; and Fig. 5*B* intermediate ventral panels).

Possible hemispheric differences in the extent of the deactivation were first assessed comparing the number of deactivated voxels in each of the hemispheres. The extent of deactivation in the left hemisphere was larger (paired one-tailed *t*-test, $P = 0.053$). Apparently, the ventral parts contributed to this hemispheric difference ($P < 0.001$ for ventral aspect only) more than the dorsal ones ($P = 0.175$). However, since no evident ventral/dorsal functional border was observed in our data (such as borders stemming from retinotopy or eccentricity mappings), the ventral/dorsal distinction for this analysis was determined according to anatomical criteria while taking into account the topography of the deactivation patches. We observed that the ventral deactivations contribute more to the functional hemispheric asymmetry than the dorsal ones; however the actual ventral–dorsal functional borders might deviate to some extent from the ones we drew. Next, a 3-way ANOVA (hemisphere, stream (ventral/dorsal), condition) on the negative signal amplitude in LG's intermediate regions (from the 4 localizer runs) showed no effect of hemisphere ($F_{1,44} < 0.34$, $P > 0.56$), but significant effects of stream (ventral > dorsal; $F_{1,44} > 9$, $P < 0.004$) and condition ($F_{3,44} > 3.5$, $P < 0.03$). The interactions were not significant (all $P$ values > 0.15). Post hoc analysis (Fisher's PLSD) for condition revealed that faces caused significantly more deactivation than houses ($P < 0.05$) and meaningless patterns ($P < 0.004$). The time courses are presented in the middle row of Figure 4.

The analysis of the time course of activity showed a tendency for a small delay in the onset of LG's hemodynamic response (Fig. 4, LG's V1 and LO panels) compared to controls. This delay is visible in the positive BOLD as well as throughout the negative BOLD regions (Fig. 4, LG intermediate dorsal and ventral panels). We assume that this difference can be attributed to hemodynamic response delays that vary between individuals and between regions within the same person (typically between 4 and 6 s), however we cannot rule out

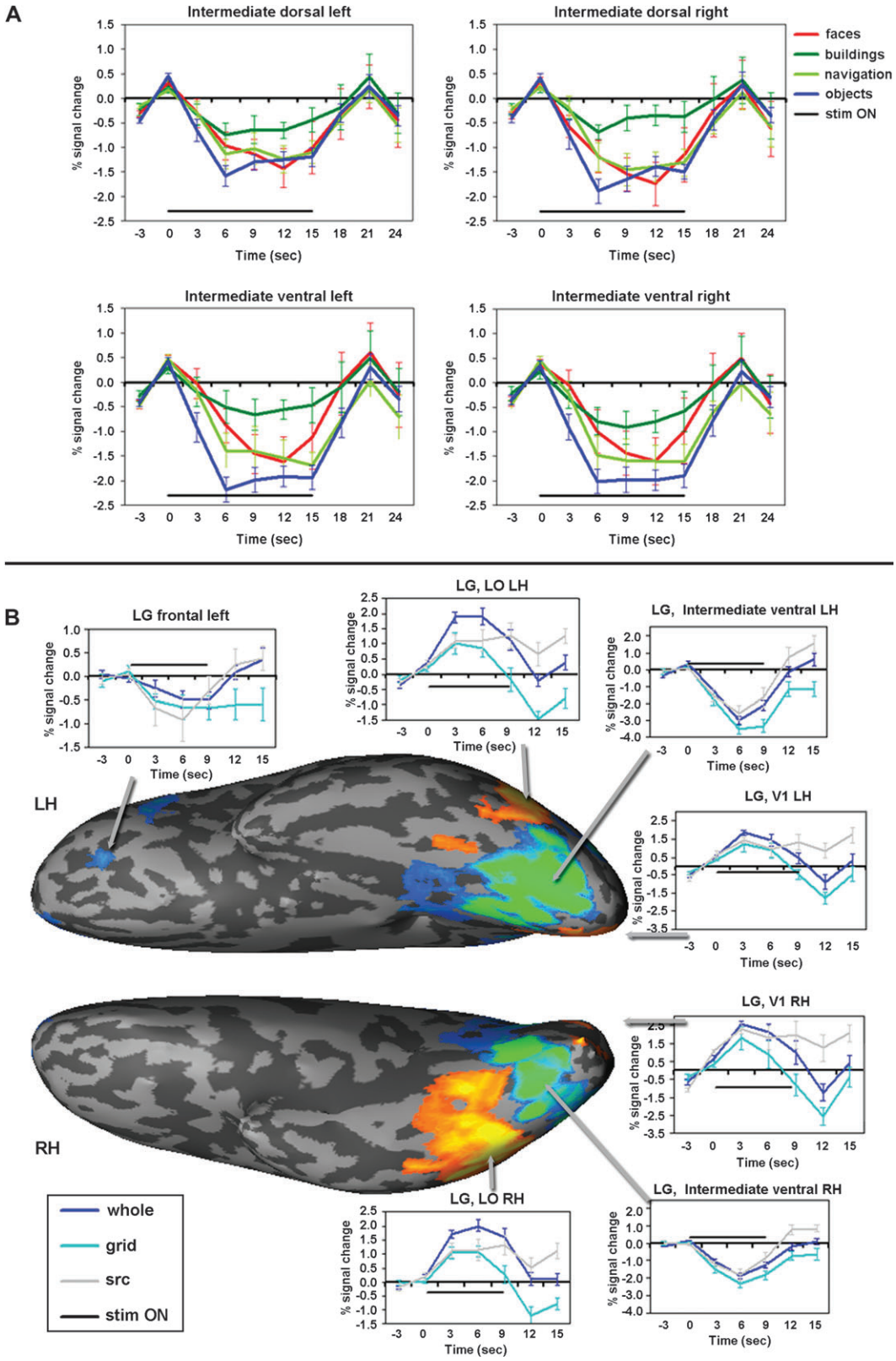


**Figure 5.** LG: Additional time courses. (*A*) Time courses from LG's intermediate deactivated regions from the category-related movie-clip experiment (Avidan et al. 2005), with block duration of 15 sec. Faces in red, buildings in green, navigation in light green, objects in blue and stimulus "ON" indicated by a black line. (*B*) Time courses from various regions in LG's cortex in the completion experiment (Lerner et al. 2001) presented along with a visual activation map. Whole indicated in blue, grid in turquoise, scrambled (scr) in gray. The activation map (same as the one presented in Fig. 3*D*) is displayed on a ventral view of LG's inflated cortical surface where the right side is the posterior part (occipital cortex) and the left is frontal cortex. LH, left hemisphere, RH, right hemisphere. Activation colors and threshold as in Figures 2 and 3. Importantly, the time courses presented here indicate that the deactivation patterns observed in LG's intermediate regions are not dependent on the stimulus duration and not dependent on the task (cf. longer deactivations (approx. 21 s) in (*A*) and deactivations in Figure 4 (approx. 12–15 s); c.f. deactivations while free viewing (*A*), naming objects (*B*), and 1-back comparison task (Fig. 4). Note also deactivated region in frontal cortex. These data indicate that the deactivations are a negative response to the visual stimulus and not a delayed hemodynamic response or a task confound.

a possibility that it reflects part of the genuine functional abnormalities in LG's visual cortex function.

More down stream in the visual cortex a significant difference in the expanse of cortical activation between the right and left hemispheres of LG showed that significantly more voxels were activated the right hemisphere than the left ($P < 0.007$, paired one-tailed *t*-test). Here too, as in the intermediate regions, it seems that the ventral aspects contribute more to this asymmetry (ventral portion only $P < 0.0005$, dorsal portion only $P = 0.175$). However, as determined by 3-way ANOVA, there was no significant difference in the response amplitude between the hemispheres, and no effect of stream ($P > 0.15$ for hemisphere, stream, and condition, $P > 0.43$ for all interactions). The time-course analysis from these areas can be seen in Figure 4 at the bottom row, as well as in Figure 5*B*. We did not directly compare the extent and amplitude of activated voxels between LG and controls because it was hard to determine the anatomical correspondence of these regions across the controls and LG (posterior border for controls). We do however present sampled time-course comparisons between LG and the control group from anatomically similar lateral occipital ventral stream visually activated regions (compare the bottom row panels in Fig. 4).

To examine whether or not the deactivations found with fMRI are due to hemodynamic temporal smearing of the neuronal response, we examined the temporal aspect of the visual response using EEG. Checkerboard patterns were presented randomly to each quadrant of the visual field, replicating the stimulus parameters and procedures previously used to localize cortical sources of the human VEP (Di Russo et al. 2002). LG and 6 age-matched controls participated in this experiment. As revealed in Figure 6, whereas the distribution and amplitudes of the C1 components, with sources reportedly localized to the calcarine cortex (V1), were fairly similar in LG and in the control group (Fig. 6*B*), their peaks in LG were significantly delayed (Fig. 6*A*). The C1 delay in LG was more salient when the stimulus was in the upper quadrants (activating the ventral banks of the calcarine sulcus), but evident in all 4 quadrants (LG: UL: 102 ms, UR: 98 ms, LL: 94 ms LR: 90 ms; Control: UL: 88 ms, UR: 85 ms, LL: 85 ms, LR: 87 ms). Relative to the distribution of the control group, the *Z*-scores of LG's latencies were UL: 2.54, UR: 1.48, LL: 2.86, and LR: 0.36. For one control participant the latencies of C1 were almost as long as for LG. This subject excluded, the LG's C1 latencies were more than 5.0 *Z*-scores from the control's distribution mean. Following C1 in time, the VEP peaks elicited in LG varied considerably from those elicited in controls, again with a more clear difference in response to stimulation of the upper quadrants. For example, the N1 components (which reportedly include generator sources in the intermediate-order visual extrastriate cortex contralateral to the stimulated field), were completely absent in LG following upper field stimulation (see Fig. 6*C*). In contrast, when the lower quadrants of the visual field were stimulated, the N1 components were elicited in LG, albeit slightly delayed when the stimuli were in the left lower quadrant.

### *Functional Organization of the Visual Pathways Beyond the Intermediate Areas*

Despite the evident disruption of the information flow in the intermediate retinotopic areas, LG's regions down stream in the visual cortex were robustly activated by visual inputs (Figs 2–5). Therefore, we further examined the functional specialization of this activation. In particular, we looked for differential activation to specific categories (faces, houses, objects), for selectivity to objects over simplified patterns (which is the hallmark of LOC; Malach et al. 1995; Grill-Spector and Malach 2004), as well as for selectivity to motion in MT+ (Huk et al. 2002; Hasson et al. 2003). As revealed in Figure 7 and in contrast to neurotypical controls (LG on right, control on the left), we did not find regions within LG's ventral stream that showed a significant selectivity to either faces (relative to the other categories) or to objects. Also, the LOC did not respond selectively to objects relative to unstructured visual patterns. Intriguingly, however, in contrast to faces and objects, regions in the CoS overlapping the PPA (Epstein and Kanwisher 1998; Levy et al. 2001), were selective to houses (contrasted with faces and objects). Moreover, normal motion selectivity was found in MT+ (see Fig. 8). In agreement with known literature, the control participants examined, with the same stimuli and fMRI sequences as LG, showed normally selective higher-level activity and organization (Figs 7 and 8, left).

The absence of significant selectivity for faces in LG's extrastriate cortex has been replicated using EEG. Like most congenital and developmental prosopagnosic patients tested so far (Kress and Daum 2003; Bentin et al. 2007), the N170 component that normally distinguishes faces from nonface stimuli was not selective in LG, however, it was similarly robust for faces and objects (see Fig. 6*D*).

A possible source for the activation in LG's ventral and dorsal visual pathways may be frontal contributions bypassing intermediate visual regions (Bar et al. 2006). We therefore examined possible responses in LG's frontal cortex for the visual stimuli. In the category-selectivity experiment we failed to find frontal responses, however we did find a deactivation focus in the orbitofrontal cortex (Talairach coordinates [*x*, *y*, *z*] = [-30, 37, 5]) in the completion experiment (Fig. 5*B* top left panel).

## Discussion

The present data demonstrate that despite significant BOLD deactivation in the intermediate visual cortex more down stream areas can be robustly activated. This evidence was obtained assessing fMRI activations in the intriguing case LG. Despite the striking interruption in the normal bottom-up cortical flow LG is able to read and copes with the visual environment as a well-adapted fully functioning independent adult, albeit he suffers from visual agnosia and severe prosopagnosia.

Whereas developmental prosopagnosia is by now amply documented in neuropsychological literature (e.g., Duchain et al. 2003; Behrmann et al. 2005; Bentin et al. 2007; DeGutis et al. 2007; for a review see Behrmann and Avidan 2005) as well as in neuroimaging (fMRI) studies (e.g., Hasson et al. 2003; Avidan et al. 2005; Behrmann et al. 2007), to our knowledge, LG is the first neuroimaging report of a *developmental object agnosic* case. Although no structural malformation was found in his brain, robust deactivations in mid-level visual areas were evident.

Critically, despite these deactivations, more down stream areas showed a robust level of fMRI activation. Furthermore, the functional mapping of these areas showed apparently

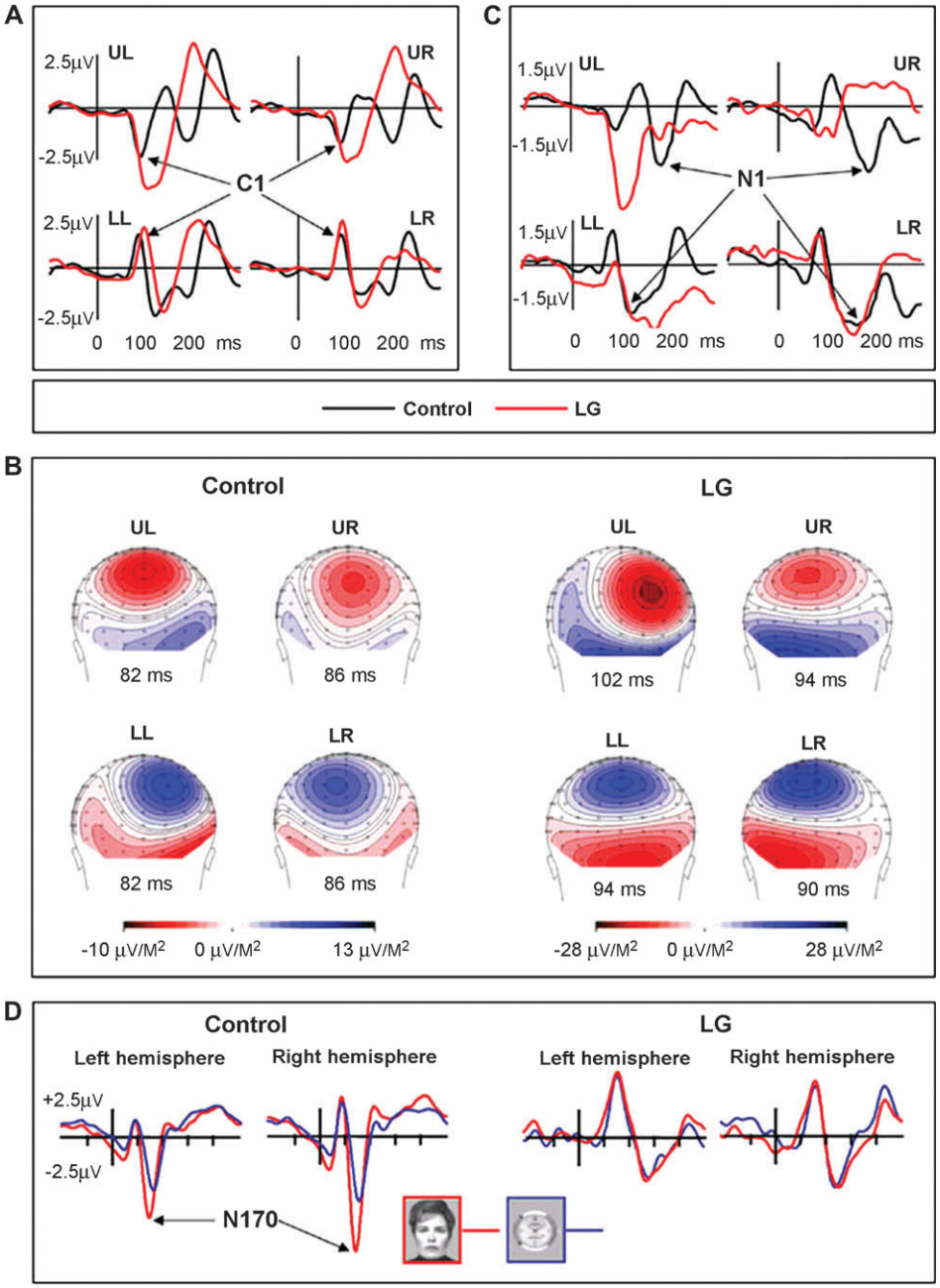


**Figure 6.** VEP and N170: LG versus controls. Electrophysiological activity elicited by LG's visual system and controls at different hierarchical levels. (*A*) V1-related C1 component: VEPs with sources in the calcarine cortex recorded at the parieto-occipital midline site (POz) in response to stimuli presented separately in the upper left (UL), upper right (UR), lower left (LL), and lower right (LR) quadrants of the visual field (Di Russo et al. 2002) (see Methods). The C1 latencies were delayed in LG relative to the controls (see Results for details). (*B*) Scalp current density (SCD) distributions at the peak of C1 elicited by stimulation in each of the four quadrants of the visual field. The sources and the sinks of the C1 dipole sources are typical for LG (right panel) and for controls. The larger amplitudes recorded in LG reflect the difference between the average of two very similar patterns within subject relative to the average of 6 participants in the control group. (*C*) The extrastriate N1 components recorded at right and left parieto-occipital sites (PO6 and PO5) (VEP experiment). The waveforms presented were recorded contralateral to the stimulated hemifield. Note the complete absence of N1 across hemifields for upper quadrants stimulation. (*D*). The high-order associated N170 component recorded at the lateral posterior-temporal sites (P9 and P10) in response to faces and watches. Note the absence of any N170-effect (that is, no special sensitivity to faces) in LG compared with the prominent normal N170-effect in the control group.

normal MT+ and CoS/PPA selectivity (for motion and houses/places, respectively). However, we found no significant selectivity to other structured stimuli within temporal-occipital regions (e.g., LOC) and impaired selectivity for faces in the fusiform. This pattern, which is in line with his performance, is intriguing both because it suggests different pathways and different selectivity constraints for the CoS and other categorically selective regions in the extrastriate cortex and because it demonstrates the extent of visual function that may reside despite striking interruption of the normal hierarchical flow of neuronal activity in the visual system.

Several mechanisms may explain the dissociation of down stream activity from low-level inputs. First, there is convincing evidence supporting bi-directional hierarchies in the visual

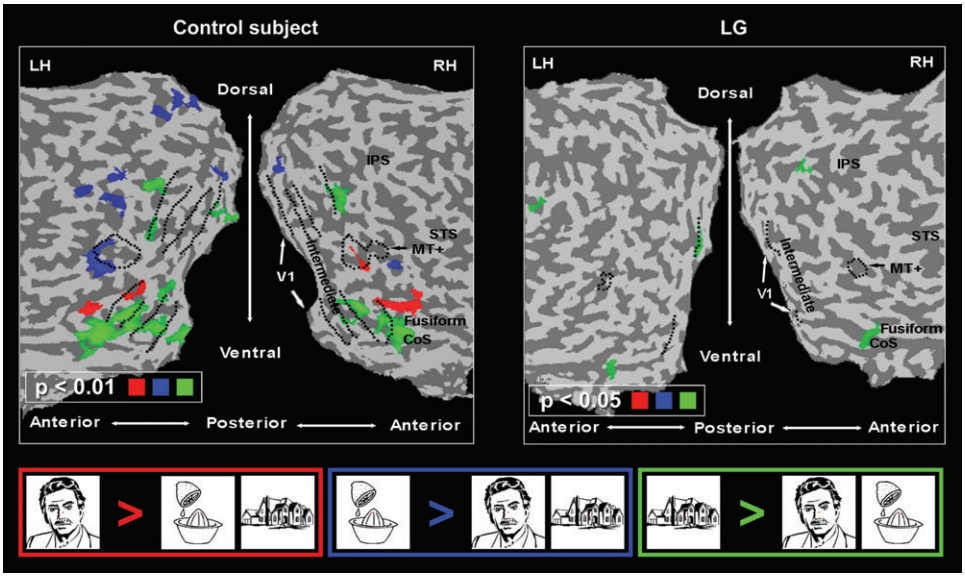


**Figure 7.** Category selectivity in high-order cortex: LG versus control. Left, typical control subject; right, LG. Same presentation format and anatomical landmarks as in Figure 2. Red represents face-selective regions; green, house selective; blue, object selective.

system (Gazzaniga et al. 2002; Hochstein and Ahissar 2002). Moreover, there are models based on fMRI and MEG data suggesting frontal and prefrontal contributions to the visual process (Bar 2003; Summerfield et al. 2006; Bar et al. 2008). Finally, the activity might be generated by a highly nonlinear local "amplification" (Douglas and Martin 2004) of inputs through the recurrent cortical circuitry (Nir et al. 2008a). Thus, the present results provide additional evidence against a view stressing primarily the straightforward bottom-up hierarchical flow of activity. Indeed, how are LG's down stream visual regions activated if regions more upstream are deactivated? One alternative then is that rapid and weak signals could still pass through intermediate cortex. Such activity might be either too weak or too sluggish to be detected by fMRI (Nir et al. 2008b). These weak inputs might be amplified by intrinsic mechanisms and connections in the higher-level areas (Raichle 2006). Another possibility is that rich and nonhierarchical interareal connectivity throughout the visual system and fronto-parietal networks (Schmolesky et al. 1998; Lamme and Roelfsema 2000; Bullier 2001b; Van Essen, 2005) could account for at least some of the visual input beyond the intermediate areas. Thus, rapid pathways from V1 to prefrontal areas could bypass or rapidly stream through the intermediate visual areas and feedback into more down stream visual regions (Bar 2003). Note, though, that our failure to find positive frontal activations in LG (Fig. 5) constraints such activation to be weak or of short duration nature. Finally, it is possible that such activity may be generated by subcortical connectivity such as thalamo-cortical connections, and reaches the visual system at all levels as suggested, for example, by the "blindsight" phenomenon (Weiskrantz 1990; Stoerig 2006) or the "Riddoch syndrome" (Riddoch 1917; Zeki and Ffytche 1998; Schoenfeld et al. 2002). (Note, however, that the role of the primary visual cortex system in the account for blindsight phenomena is not finally settled; Stoerig 2006.) Indeed, recent studies suggest that the pulvinar sends and receives information from all levels of the visual cortex in parallel (Van Essen, 2005).

A slightly different question is raised by finding selectivity for houses and places with impaired or absent selectivity for faces and other objects. Since the same tasks were used to localize selective activity across all stimulus categories it is very unlikely that task demands could account for this differential selectivity along the ventral visual pathway. A possible alternative explanation could be that the house and place selectivity was spared in LG because the processing of houses and places involves more peripheral retinotopic areas, which integrate information over larger fields (Levy et al. 2004). According to this interpretation, the visual input that reached the regions down stream from V2 to V4 in LG was sufficient for selective processing of stimuli which do not require high visual resolution for recognition, but not for stimuli that require more detailed visual analysis such as faces and small objects (Levy et al. 2001). This interpretation implies that the information provided by the coarser resolution of the retinal periphery is more resilient to disruptions in the bottom-up flow than is the more detailed information required to process faces and objects which might be more dependent on foveal information. An analogous phenomenon has been recently reported in the case of amblyopia (Lerner et al. 2003). It has been suggested that the parahippocampal cortex, apart from processing visual place information, plays a role in episodic memory (Gabrieli et al. 1997; Brewer et al. 1998; Schacter and Wagner 1999) and processes contextual associations, even when the associations are not spatial (Aminoff et al. 2007; Bar et al. 2008). Therefore, the selectivity found in LG's parahippocampal region may perhaps be attributed to the putative role of this region in forming associations. Similarly, the apparently normal selectivity to motion observed in LG could be accounted for by direct connectivity between V1 and MT+ (Maunsell and Newsome 1987; Felleman and Van Essen 1991). In other words, the present data suggest that proper integration of features in the intermediate visual cortex is essential for discriminating details and, consequently, for the preferential activation of object- and face-selective regions in the ventral pathway of the visual system, but less essential for

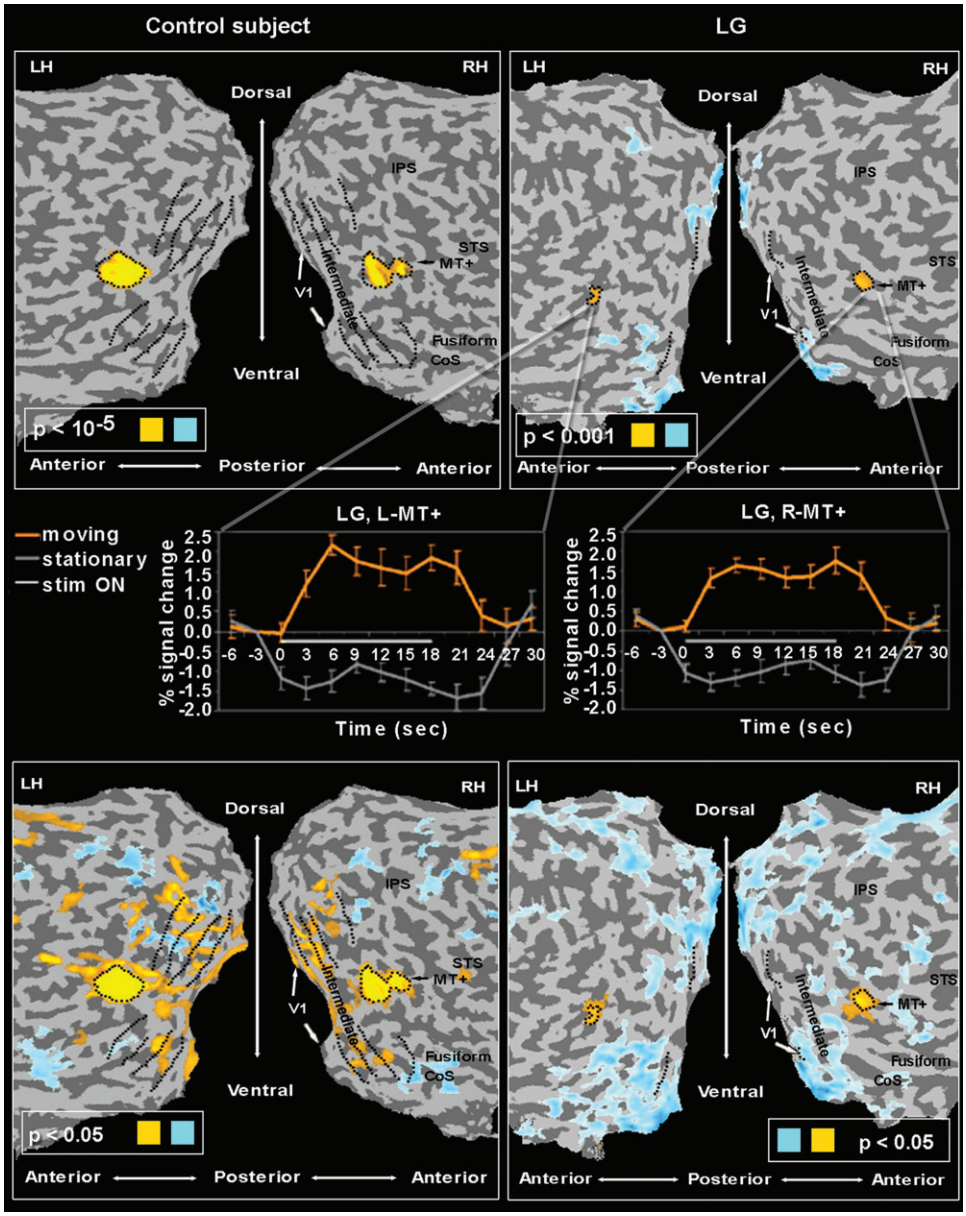


**Figure 8.** Motion sensitivity in LG versus control. Same presentation format and anatomical landmarks as in Figure 2 (LG, right, control, left). Yellow indicates motion-sensitive voxels (test: motion > static; Hasson et al. 2003), light blue indicates static preference (static > motion). Motion sensitivity was found in LG in the expected MT+ location (top panels maps set at high threshold). These maps at high threshold indicate the MT+ ROI definition. At lower threshold, however, this motion sensitivity in LG did not expand beyond MT+, as typically found in controls (bottom panels maps set at lower threshold). The average time courses of LG's right and left MT+ (as sampled from the motion-selectivity experiment) are presented in the mid pannels (orange indicates response to motion blocks, gray indicates response to static blocks).

the preferential activation of house-selective regions. Supporting this conceptualization, LG's performance is largely compatible with the selectivities developed in his visual cortex. Specifically, his recognition of famous or personally familiar places from pictures as well as his ability to navigate are much better than his ability to identify objects and familiar people's faces. On the other hand, LG's evident reading ability (which also requires processing of details) is not in line with this interpretation. Therefore, it would be interesting in the future to test this concept even further and look for letter and word specializations (Hasson et al. 2002) in LG's visual cortex.

In addition to interrupting the informational flow downstream, we should also briefly consider the possible consequences of the profound deactivation of intermediate areas on feedback loops from more down stream regions in the visual cortex (and beyond), upstream. For example, it has been suggested that V1 could be modulated directly by top-down activity during spatial attention tasks (e.g., Brefczynski and DeYoe 1999; Somers et al. 1999). Furthermore, such effects were demonstrated even in the absence of visual stimuli, likely reflecting expectation effects (Ress et al. 2000). It is an intriguing question whether such top-down effects may still be present and active in LG, despite the mid-level interruption. However, additional research will be needed to address this interesting issue.

What could account for the negative BOLD signal found in LG's intermediate regions, instead of the expected positive

BOLD? One possibility is that the source of this negative BOLD signal is, in fact, not neuronal. However, this possibility is unlikely in light of recent evidence that links decreased neuronal activity and negative BOLD signal (Shmuel et al. 2006). Moreover, the electrophysiological findings in the present study also speak against this possibility since ERPs, unlike fMRI, are a direct reflection of neuronal activity. Despite their delayed latencies, the normally distributed robust C1 components elicited in LG, which were localized by dipole modeling in, or close to V1 (Di Russo et al. 2002), and the gross abnormality in later extrastriate ERP components (N1) support a neuronal origin for the abnormal cortical behavior primarily (even if not solely) in the extrastriate cortex as was revealed by fMRI.

Although the spatio-temporal low-pass nature of the hemodynamic response prevents a clear-cut account for the neuronal mechanism underlying the negative BOLD in LG's intermediate visual cortex, assuming that it has a neuronal source, one can envision three alternative scenarios that may lead to reduced fMRI signals. The most straightforward possibility is that, indeed, due to some aberrant anatomical/developmental mechanisms, the neuronal activity in this region is completely shut off. This could result, for example, if inputs from V1 would target only inhibitory neurons in mid-level areas. Yet this account leaves open the question of where do the excitatory inputs to more down stream visual areas come from. As discussed above, these inputs could originate from parallel thalamo-cortical pathways such as the one putatively implicated in the blindsight phenomenon (Stoerig 2006). Although demonstrating a major functional abnormality in LG's visual cortex (at a spatial resolution of $3 \times 3 \times 5$ mm$^3$), the examination of his structural data (spatial resolution of $1 \times 1 \times 1$ mm$^3$) did not reveal any evident brain lesions or discernible structural cortical abnormality. Thus, at this stage and with the current measuring resolution, our data cannot support or rule out this scenario.

A second alternative is that a residual excitatory neuronal activity remained in the deactivated areas, however this activity was too sparse to generate a positive BOLD. For example, it is possible that due to lateral inhibitory interactions, the few activated neurons lead to a large scale inhibition among the majority of neurons in the vicinity and, consequently, the net neuronal activity is reduced. Finally, it could be that a very rapid wave of activity, of the type that may travel rapidly from V1 all-the-way to frontal cortex (Bar et al. 2006) is first sweeping through the entire visual hierarchy, including the "inhibited" mid-tier areas. A longer lasting wave of inhibition could reduce the activity in these areas at a second stage. According to the latter account, the fact that the fMRI signal averages the responses over time may hinder the detection of such rapid, transient responses. Some evidence against this "dynamic" account is provided by the prolonged C1 latencies and abnormal N1 found in LG's VEP that are sensitive to fast activity transients. As mentioned above, several authors reported that the N1 has a source in the intermediate cortex. Magnocellular and parvocellular inputs to the visual cortex are likely to play a role in such a case. Magnocellular cortical inputs are associated with motion and contrast processing and are considered to play an important role in dorsal stream input, whereas parvocellular inputs are associated with shape and color processing and are dominant in ventral stream processing. Schmolesky et al. (1998) reported that the magnocellular stream displays shorter latencies and travels through the visual system more rapidly and uniformly than the parvocellular stream. They also suggest that magnocellular stream could modulate parvocellular processing. Taken together, this pattern might indicate that LG's magnocellular cortical inputs stream rapidly through the hierarchy and yet the later parvocellular-stream processing is abnormal.

Although this was not the main focus of our study, it is interesting to compare the V1 activation in LG with that of control participants. Although LG's V1 showed a robust and significant activation amplitude to all visual stimuli it should be emphasized that this does not prove that the functional profile of V1 was completely normal. The important point with regards to simple hierarchical models, is that despite this large amplitude activation impinging on intermediate cortex, these receiving areas in intermediate cortex actually showed signal *deactivation*. Such sign inversion argues against simple feed-forward hierarchical models in which down stream areas simply reflect and "process" the information coming from earlier stages. Instead, these results suggest that neuronal activation, although affected by cortical inputs, is not a mere reflection of such inputs, but is generated "de novo" by local amplification processes in each cortical region. As reported above, the C1 component of the VEP, which has sources in V1 was delayed relative to control participants suggesting some abnormality. Yet it was normally distributed suggesting that stimulation of all 4 quadrants in the visual field triggered responses in both the upper and the lower banks of the calcarine cortex in both hemispheres. Moreover, we have observed a similar delay in 1 out of 6 control participants. The interindividual variance was even more conspicuous in the extent of activated V1, as well as differences within LG in the different runs. We note that high interindividual variability in size variance of V1 in normal population (up to three-fold difference between individuals) is a well documented phenomemnon (e.g., post-mortem studies: Stensaas et al. 1974; Andrews et al. 1997; Adams et al. 2007; Amunts et al. 2007; and fMRI: Dougherty et al. 2003). The study by Dougherty and colleagues (Dougherty et al. 2003) is particularly relevant to the present study since the measurements were done *in vivo* using fMRI, and the stimuli were of comparable size (12°). In controls, assuming a 2 mm cortical thickness we found the size of left V1 to be 522 mm$^2$ on average (LG: 526 mm$^2$) while Dougherty and colleagues report on 936–2271 mm$^2$ with an average of 1578 mm$^2$. For the right V1 we measured 525 mm$^2$ in controls (LG: 465 mm$^2$) versus Dougherty and colleagues reporting on 1074–1813 mm$^2$ with an average of 1362 mm$^2$. We believe that the difference between the extent of activated V1 cortex we and the Dougherty paper report on originates from the nature of the stimuli. Dougherty applied rotating and expanding checkerboard stimuli best suited to activate V1 preferentially, while in our study we report on activated cortex to line drawings which are less optimal for V1. Interestingly, the crowding effects which were observed in LG are commonly attributed to extrastriate intermediate visual processing mechanisms beyond V1 (He et al. 1996). Hence, these effects could, in fact, partially reflect the negative BOLD signal that was measured in LG's intermediate cortex in response to visual stimuli. We are currently working on investigating the source and nature of this deactivation. Finally, it is intriguing to note that the functional abnormality observed in LG's visual cortex activations was not symmetrical across hemispheres and was not symmetrical across the vertical dimension. The

abnormality observed in the ventral aspects of both hemispheres was higher than in the dorsal parts, in line with his relative higher impairment in the identification of objects and faces as opposed to navigation and recognition of places and houses. In line with this ventral–dorsal asymmetry the prolonged latency and enhanced amplitude of the C1 potentials recorded in LG relative to controls were more conspicuous in response to upper field than to lower field stimulation. Since upper field stimuli are associated with ventral stream processing at early and intermediate retinotopic regions, this again indicates that LG's intermediate level abnormalities were greater in ventral than dorsal visual areas. Further, we found higher functional damage in the left hemisphere than in the right hemisphere. The right-left asymmetry is particularly interesting given that LG's language ability is high, including normal reading. This pattern is reminiscent of cases with infantile hemiplegia that preserve relative normal language function regardless of whether the spared hemisphere was right or left (Kohn and Dennis 1974; Bishop 1993). The interhemispheric asymmetrical pattern might also be related to current developmental studies indicating that the development of face recognition performance correlates with the development of the FFA in the right hemisphere whereas the development of houses and places recognition develops in correlation with the development of the PPA in the left hemisphere (Golarai et al. 2007). In conclusion, we have shown that in LG's visual cortex, despite strong activity of the inputs to mid-level cortex (as reflected by the high activity of V1), mid-cortex is deactivated, and despite the deactivation of inputs to high-level cortex (as reflected by the deactivation of V2 and V3/VP) these regions nevertheless show strong activation (robust activation of LOC, MT+, and intraparietal regions). Hence, the cortical activation in LG's visual system indicates that high-level visual areas such as LOC, MT+, and intraparietal regions can be robustly activated even when the building blocks that they rely on are substantially deactivated (regions V2 and V3/VP). The main consequence of this hierarchical disruption is the fact that category-selective regions relying on high-resolution foveally biased information fail to function properly. This pattern suggests that intermediate visual areas play an essential role in the creation of selective activity in the visual cortex, especially for foveally mid-biased object categories (Levy et al. 2001; Hasson et al. 2003). Moreover, the robust activity and residual selectivity in the ventral and dorsal visual pathways suggests that not all visual performance depends on similar hierarchical processing sequences.

## Supplementary Material

Supplementary material can be found at: http://www.cercor.oxfordjournals.org/


## Funding

NIMH grant (R01 MH 64458) to S.B.; ISF grant; Benoziyo Center for Neurodegenerative Disorders, and Dominique Center, and the Minerva Foundation to Rafael Malach.

## Notes

We thank LG and his family, the Wohl Imaging unit in Sourasky Medical Center headed by Dr Talma Hendler, and Daniel Rosenblatt and Ida Sivan. We thank Ifat Levy for her great support with the experimental setup and data collection. We thank Michal Harel for the brain reconstruction and flattening procedure. We thank Uri Polat for comments on the manuscript. *Conflict of Interest*: None declared.



Address correspondence to Shlomo Bentin, PhD, Department of Psychology, Hebrew University of Jerusalem, Jerusalem 91905, Israel. Email: shlomo.bentin@huji.ac.il.


## References


Adams DL, Sincich LC, Horton JC. 2007. Complete pattern of ocular dominance columns in human primary visual cortex. J Neurosci. 27:10391–10403.

Aminoff E, Gronau N, Bar M. 2007. The parahippocampal cortex mediates spatial and nonspatial associations. Cereb Cortex. 17:1493–1503.

Amunts K, Armstrong E, Malikovic A, Hömke L, Mohlberg H, Schleicher A, Zilles K. 2007. Gender-specific left-right asymmetries in human visual cortex. J Neurosci. 27:1356–1364.

Andrews TJ, Halpern SD, Purves D. 1997. Correlated size variations in human visual cortex, lateral geniculate nucleus, and optic tract. J Neurosci. 17:2859–2868.

Ariel R, Sadeh M. 1996. Congenital visual agnosia and prosopagnosia in a child: a case report. Cortex. 32:221–240.

Avidan G, Harel M, Hendler T, Ben-Bashat D, Zohary E, Malach R. 2002. Contrast sensitivity in human visual areas and its relationship to object recognition. J Neurophysiol. 87:3102–3116.

Avidan G, Hasson U, Malach R, Behrmann M. 2005. Detailed exploration of face-related processing in congenital prosopagnosia: 2. Functional neuroimaging findings. J Cogn Neurosci. 17:1150–1167.

Bar M. 2003. A cortical mechanism for triggering top-down facilitation in visual object recognition. J Cogn Neurosci. 15:600–609.

Bar M, Aminoff E, Ishai A. 2008. Famous faces activate contextual associations in the parahippocampal cortex. Cereb Cortex. 18:1233–1238.

Bar M, Kassam KS, Ghuman AS, Boshyan J, Schmid AM, Dale AM, Hämäläinen MS, Marinkovic K, Schacter DL, Rosen BR, et al. 2006. Top-down facilitation of visual recognition. Proc Natl Acad Sci USA. 103:449–454.

Barton JJ, Press ZP, Keenan JP, O'Connor M. 2002. Lesions of the fusiform face area impair perception of facial configuration in prosopagnosia. Neurology. 58:71–78.

Behrmann M, Avidan G. 2005. Congenital prosopagnosia: face-blind from birth. Trends Cogn Sci. 9:180–187Review.

Behrmann M, Avidan G, Gao F, Black S. 2007. Structural imaging reveals anatomical alterations in inferotemporal cortex in congenital prosopagnosia. Cereb Cortex. 17:2354–2363.

Behrmann M, Avidan G, Marotta JJ, Kimchi R. 2005. Detailed exploration of face-related processing in congenital prosopagnosia: 1. Behavioral findings. J Cogn Neurosci. 17:1130–1149.

Bentin S, Allison T, Puce A, Perez E, McCarthy G. 1996. Electrophysiological studies of face perception in humans. J Cogn Neurosci. 8:551–565.

Bentin S, Degutis JM, D'Esposito M, Robertson LC. 2007. Too many trees to see the forest: performance, event-related potential, and functional magnetic resonance imaging manifestations of integrative congenital prosopagnosia. J Cogn Neurosci. 19:132–146.

Bentin S, Deouell LY, Soroker N. 1999. Selective visual streaming in face recognition: evidence from developmental prosopagnosia. Neuroreport. 10:823–827.

Benton AL, Sivan AB, Hamsher KdeS, Varney NR, Spreen O. 1983. Contribution to neuropsychological assessment. New York: Oxford University Press.

Bishop D. 1993. Language Development after Focal Brain Damage. In: Bishop D, Mogford K, editors. Language Development in exceptional circumstance. Hove (UK): Lawrence Erlbaum Associates. p. 203–219.

Bonneh YS, Sagi D, Polat U. 2004. Local and non-local deficits in amblyopia: acuity and spatial interactions. Vision Res. 44: 3099–3110.

Bouvier EE, Engel SA. 2006. Behavioral deficits and cortical damage loci in cerebral achromatopsia. Cereb Cortex. 16:183–191.
Brefczynski JA, DeYoe EA. 1999. A physiological correlate of the 'spotlight' of visual attention. Nat Neurosci. 2:370–374.
Brewer JB, Zhao Z, Desmond JE, Glover GH, Gabrieli JD. 1998. Making memories: brain activity that predicts how well visual experience will be remembered. Science. 281:1185–1187.
Bullier J. 2001a. Feedback connections and conscious vision. Trends Cogn Sci. 5:369–370.
Bullier J. 2001b. Integrated model of visual processing. Brain Res Brain Res Rev. 36:96–107. Review.
Cowey A. 1994. Cortical visual areas and the neurobiology of higher visual processes. In: Farah MJ, Ratcliff G, editors. The neuropsychology of high-level vision: collected tutorial essays. Hillsdale (NJ): Lawrence Erlbaum Associates.
Davidoff J, Warrington EK. 1999. Apperceptive agnosia: a deficit of perceptual categorization of objects. In: Humphreys GW, editor. Case studies in the neuropsychology of vision. Hove (UK): Psychology Press.
De Haan EH, Campbell R. 1991. A fifteen year follow-up of a case of developmental prosopagnosia. Cortex. 27:489–509.
DeGutis JM, Bentin S, Robertson LC, D'Esposito M. 2007. Functional plasticity in ventral temporal cortex following configural training with faces in a congenital prosopagnosic. J Cogn Neurosci. 19:1790–1802.
DeYoe EA, Carman GJ, Bandettini P, Glickman S, Wieser J, Cox R, Miller D, Neitz J. 1996. Mapping striate and extrastriate visual areas in human cerebral cortex. Proc Natl Acad Sci USA. 93: 2382–2386.
Di Russo F, Martinez A, Sereno MI, Pitzalis S, Hillyard SA. 2002. Cortical sources of the early components of the visual evoked potential. Hum Brain Mapp. 15:95–111.
Dougherty RF, Koch VM, Brewer AA, Fischer B, Modersitzki J, Wandell BA. 2003. Visual field representations and locations of visual areas V1/2/3 in human visual cortex. J Vis. 3:586–598.
Douglas RJ, Martin KA. 2004. Neuronal circuits of the neocortex. Annu Rev Neurosci. 27:419–451. Review.
Duchaine B, Nakayama K. 2006. The Cambridge Face Memory Test: results for neurologically intact individuals and an investigation of its validity using inverted face stimuli and prosopagnosic patients. Neuropsychologia. 44:576–585.
Duchaine BC, Parker H, Nakayama K. 2003. Normal recognition of emotion in a prosopagnosic. Perception. 32:827–838.
Engel SA, Glover GH, Wandell BA. 1997. Retinotopic organization in human visual cortex and the spatial precision of functional MRI. Cereb Cortex. 7:181–192.
Epstein R, Kanwisher N. 1998. A cortical representation of the local visual environment. Nature. 392:598–601.
Farah M. 1990. Visual agnosia: disorders of object recognition and what they tell us about normal vision. Cambridge (MA): MIT Press.
Felleman DJ, Van Essen DC. 1991. Distributed hierarchical processing in the primate cerebral cortex. Cereb Cortex. 1:1–47.
Friston KJ, Holmes AP, Worsley KJ, Poline JB, Frith C, Frackowiak RSJ. 1995. Statistical parametric maps in functional imaging: a general linear approach. Hum Brain Mapp. 2:189–210.
Gabrieli JDE, Brewer JB, Desmond JE, Glover GH. 1997. Separate neural bases of two fundamental memory processes in the human medial temporal lobe. Science. 276:264–266.
Gazzaniga MS, Ivry RB, Mangun GR. 2002. the biology of the mind. Cognitive neuroscience. 2nd ed.. New York (NY): W.W. Norton & Company.
Golarai G, Ghahremani DG, Whitfield-Gabrieli S, Reiss A, Eberhardt JL, Gabrieli JD, Grill-Spector K. 2007. Differential development of high-level visual cortex correlates with category-specific recognition memory. Nat Neurosci. 10:512–522.
Grill-Spector K, Malach R. 2004. The human visual cortex. Annu Rev Neurosci. 27:649–677.
Halgren E, Dale AM, Sereno MI, Tootell RBH, Marinkovic K, Rosen BR. 1999. Location of human face-selective cortex with respect to retinotopic areas. Hum Brain Mapp. 7:29–37.
Hasson U, Harel M, Levy I, Malach R. 2003. Large-scale mirror-symmetry organization of human occipito-temporal object areas. Neuron. 37:1027–1041.
Hasson U, Levy I, Behrmann M, Hendler T, Malach R. 2002. Eccentricity bias as an organizing principle for human high-order object areas. Neuron. 34:479–490.
He S, Cavanagh P, Intriligator J. 1996. Attentional resolution and the locus of visual awareness. Nature. 383:334–337.
Heider B. 2000. Visual form agnosia: Neural mechanisms and anatomical foundations. Neurocase. 6:1–12.
Hochstein S, Ahissar M. 2002. View from the top: hierarchies and reverse hierarchies in the visual system. Neuron. 36:791–804.
Hubel DH, Wiesel TN. 1998. Early exploration of the visual cortex. Neuron. 20:401–412.
Huk AC, Dougherty RF, Heeger DJ. 2002. Retinotopy and functional subdivision of human areas MT and MST. J Neurosci. 22:7195–7205.
Jones RD, Tranel D. 2001. Severe developmental prosopagnosia in a child with superior intellect. J Clin Exp Neuropsychol. 23:265–273.
Joy P, Brunsdon R. 2002. Visual agnosia and prosopagnosia in childhood: a prospective case study. Child Neuropsychol. 8:1–15.
Kanwisher N, McDermott J, Chun MM. 1997. The fusiform face area: a module in human extrastriate cortex specialized for face perception. J Neurosci. 17:4302–4311.
Kastner S, De Weerd P, Pinsk MA, Elizondo MI, Desimone R, Ungerleider LG. 2001. Modulation of sensory suppression: implications for receptive field sizes in the human visual cortex. J Neurophysiol. 86:1398–1411.
Kohn B, Dennis M. 1974. Patterns of hemispheric specialization after hemidecortication for Infantile Hemiplegia. In: Kinsborne M, Smith WL, editors. Hemispheric disconnection and cerebral function. Springfield (IL): Charles C Thomas Publishers. p. 5–33.
Kovacs I, Kozma P, Feher A, Benedek G. 1999. Late maturation of visual spatial integration in humans. Proc Natl Acad Sci USA. 96:12204–12209.
Kress T, Daum I. 2003. Event-related potentials reflect impaired face recognition in patients with congenital prosopagnosia. Neurosci Lett. 352:133–136.
Lamme VA, Roelfsema PR. 2000. The distinct modes of vision offered by feedforward and recurrent processing. Trends Neurosci. 23:571–579. Review.
Lerner Y, Hendler T, Ben-Bashat D, Harel M, Malach R. 2001. A hierarchical axis of object processing stages in the human visual cortex. Cereb Cortex. 11:287–297.
Lerner Y, Hendler T, Malach R. 2002. Object-completion effects in the human lateral occipital complex. Cereb Cortex. 12:163–177.
Lerner Y, Pianka P, Azmon B, Leiba H, Stolovitch C, Loewenstein A, Harel M, Hendler T, Malach R. 2003. Area-specific amblyopic effects in human occipitotemporal object representations. Neuron. 40:1023–1029.
Levy I, Hasson U, Avidan G, Hendler T, Malach R. 2001. Center-periphery organization of human object areas. Nat Neurosci. 4:533–539.
Levy I, Hasson U, Harel M, Malach R. 2004. Functional analysis of the periphery effect in human building related areas. Hum Brain Mapp. 22:15–26.
Malach R, Reppas JB, Benson RR, Kwong KK, Jiang H, Kennedy WA, Ledden PJ, Brady TJ, Rosen BR, Tootell RB. 1995. Object-related activity revealed by functional magnetic resonance imaging in human occipital cortex. Proc Natl Acad Sci USA. 92:8135–8139.
Maunsell JHR, Newsome WT. 1987. Visual processing in monkey extrastriate cortex. Annu Rev Neurosci. 10:363–401.
McConachie HR. 1976. Developmental prosopagnosia. A single case report. Cortex. 12:76–82.
Nir Y, Dinstein I, Malach R, Heeger DJ. 2008. BOLD and spiking activity. Nat Neurosci. 11:523–524.
Nir Y, Mukamel R, Dinstein I, Privman E, Harel M, Fisch L, Gelbard-Sagiv H, Kipervasser S, Andelman F, Neufeld MY, et al. 2008. Interhemispheric correlations of slow spontaneous neuronal fluctuations revealed in human sensory cortex. Nat Neurosci. 11:1100–1108.
Navon D. 1977. Forest before trees: The precedence of global features in visual perception. Cogne Psychol. 9:353–383.

Oldfield RC. 1971. The assessment and analysis of handedness: The Edinburgh inventory. Neuropsychologia. 9:97–114.
Polat U, Sagi D. 1993. Lateral interactions between spatial channels: suppression and facilitation revealed by lateral masking experiments. Vision Res. 33:993–999.
Raichle ME. 2006. Neuroscience. The brain's dark energy. Science. 314:1249–1250.
Ress D, Backus BT, Heeger DJ. 2000. Activity in primary visual cortex predicts performance in a visual detection task. Nat Neurosci. 3:940–945.
Riddoch G. 1917. Dissociation of visual perceptions due to occipital injuries, with especial reference to appreciation of movement. Brain. 40:15–57.
Riddoch MJ, Humphreys GW. 1993. BORB: Birmingham Object Recognition Battery. Hove (UK): Lawrence Erlbaum Associates.
Schacter DL, Wagner AD. 1999. Medial temporal lobe activations in fMRI and PET studies of episodic encoding and retrieval. Hippocampus. 9:7–24. Review.
Schmolesky MT, Wang Y, Hanes DP, Thompson KG, Leutgeb S, Schall JD, Leventhal AG. 1998. Signal timing across the macaque visual system. J Neurophysiol. 79:3272–3278.
Schoenfeld MA, Noesselt T, Poggel D, Tempelmann C, Hopf JM, Woldorff MG, Heinze HJ, Hillyard SA. 2002. Analysis of pathways mediating preserved vision after striate cortex lesions. Ann Neurol. 52:814–824.
Sereno MI, Dale AM, Reppas JB, Kwong KK, Belliveau JW, Brady TJ, Rosen BR, Tootell RB. 1995. Borders of multiple visual areas in humans revealed by functional magnetic resonance imaging. Science. 268:889–893.
Shmuel A, Augath M, Oeltermann A, Logothetis NK. 2006. Negative functional MRI response correlates with decreases in neuronal activity in monkey visual area V1. Nat Neurosci. 9:569–577.
Smith AT, Singh KD, Williams AL, Greenlee MW. 2001. Estimating receptive field size from fMRI data in human striate and extrastriate visual cortex. Cereb Cortex. 11:1182–1190.
Somers DC, Dale AM, Seiffert AE, Tootell RB. 1999. Functional MRI reveals spatially specific attentional modulation in human primary visual cortex. Proc Natl Acad Sci USA. 96:1663–1668.
Stensaas SS, Eddington DK, Dobelle WH. 1974. The topography and variability of the primary visual cortex in man. J Neurosurg. 40:747–755.
Stoerig P. 2006. Blindsight, conscious vision, and the role of primary visual cortex. Prog Brain Res. 155:217–234. Review.
Summerfield C, Egner T, Greene M, Koechlin E, Mangels J, Hirsch J. 2006. Predictive codes for forthcoming perception in the frontal cortex. Science. 314:1311–1314.
Talairach J, Tournoux P. 1988. Co-planar stereotaxic atlas of the human brain. New York: Thieme Medical Publishers.
Tootell RB, Dale AM, Sereno MI, Malach R. 1996. New images from human visual cortex. Trends Neurosci. 19:481–489.
Ungerleider LG, Mishkin M. 1982. Two cortical visual systems. In: Ingle DJ, Goodale MA, Mansfield RJW, editors. Analysis of visual behavior. Cambridge (MA): MIT Press. p. 549–586.
Van Essen DC. 2005. Corticocortical and thalamocortical information flow in the primate visual system. Prog Brain Res. 149:173–185.
Warrington E. 1984. Recognition memory test manual. Windsor (UK): Nelson.
Weiskrantz L. 1990. The Ferrier lecture, 1989. Outlooks for blindsight: explicit methodologies for implicit processes. Proc R Soc Lond B Biol Sci. 239:247–278.
Zeki S, Ffytche DH. 1998. The Riddoch syndrome: insights into the neurobiology of conscious vision. Brain. 121:25–45.